Extending the Magnitude Range of Seismic Reservoir Monitoring by Utilizing Hybrid Surface – Downhole Seismic Networks*

Gisela Viegas[1], Katherine Buckingham[2], Anisa Kassam[2], Margaret Seibel[2], Adam Baig[2], and Ted Urbancic[2]

Search and Discovery Article #41285 (2014)
Posted March 10, 2014

*Adapted from extended abstract prepared in conjunction with presentation at CSPG/CSEG/CWLS GeoConvention 2012, (Vision) Calgary TELUS Convention Centre & ERCB Core Research Centre, Calgary, AB, Canada, 14-18 May 2012, AAPG/CSPG©2014

[1]ESG, Kingston, Ontario, Canada (Gisela.Fernandes@esgsolutions.com)
[2]ESG, Kingston, Ontario, Canada

Abstract

We analyze seismicity recorded over the full range from –M3 to M3 as related to a water flood injection program in a carbonate hydrocarbon reservoir at ~2 km depth. Data is recorded with a hybrid monitoring seismic network comprised of downhole arrays of 4.5 Hz and 15 Hz omni-directional triaxial geophones and surface stations consisting of force balance accelerometers to increase the dynamic range of recordable signals. We analyze the seismic characteristics of these events with two goals in sight, first to assess and improve the reservoir monitoring networks capability, and second to understand the underlying generation mechanism of the larger local events. Understanding the network capability and the reservoir seismicity is fundamental towards an improved reservoir management system.

Introduction

Seismic networks deployed to monitor production related activity in reservoirs are designed to detect and analyze micro-earthquakes at very short distances. In particular hydraulic fracturing and cyclic steam injection activities generate thousands of micro-earthquakes with magnitudes in the range of -M4 to -M1. These networks are generally set-up to record high frequency signals and use time records with a short duration. However, these networks are not ideal for analyzing larger magnitude events, typically ranging from M0 to M3: there is not enough low frequency signal recorded and the pre-set time windows are generally too short to contain both P and S arrivals.

We monitor the seismicity at a hydrocarbon reservoir during a one-year period as related to a water flood injection program. The majority of the reservoir events have magnitudes between –M2 to M1. However a few M2 macro-events were observed. These larger events are irregular in this region and we investigate their mechanism and possible cause. For that we use an array composed of vertical borehole toolstrings enhanced with longer period surface stations to record broadband signals.

Seismic Network

The network consists of 11 downhole vertical observation wells each with 8 levels with alternating 4.5 Hz and 15 Hz three component omni-directional geophones. The vertical observation wells have variable depths, with the maximum depth of 400 m. The seismic network is complemented/enhanced with 4 surface force balance accelerometers and is spread over a surface area of approximatelly140 km^2. Recording time windows vary depending on the sensor type. Geophones use 6.5 second windows and the accelerometers use windows varying from 1 to 5 minutes, depending on the event duration so that both P and S wave arrivals of larger more distant events are recorded.

Hydrocarbon Reservoir Seismicity

The hydrocarbon reservoir consists of a sandstone and shale gas reservoir overlying a carbonate oil reservoir. There is ongoing gas production above the oil bearing layers where water is being injected. The gas production has been driven by natural depletion and the gas reservoir pressure has largely decreased since the onset of production more than two decades ago. The reservoir depletion was accompanied by surface subsidence, as is often the case (Figure 1). There are no records of felt earthquakes in the region prior to the beginning of hydrocarbon production.

Seismicity at the hydrocarbon reservoir was monitored for a period of one year. An average of 100 microseismic events per month have been detected, with magnitudes ranging from -M2 to M3, with less than 3% of the micro-earthquakes being larger than M1. The microseismicity is mainly located along pre-existing reservoir faults (a set of conjugated predominantly high angle normal faults) and is relatively shallow (~ 1 km) and located above the depth at which water is being injected (~2 km). The micro-earthquake locations and depths are consistent with locations obtained in previous microseismic studies of the hydrocarbon reservoir (Kuleli et al., 2009) where micro-earthquakes were also found to occur predominately in the gas reservoir on pre-existing faults. Li et al. (2011) analyzed micro-earthquakes (-M1 to M1) recorded between 1999 and 2007 in this reservoir and found a dominant normal faulting mechanism with the majority of the events having a strike direction parallel with the major faults in the region. Li et al. (2011) proposed that the vertical stress is larger than the horizontal stress in the reservoir area, because of the predominance of the normal faulting mechanism.

The dataset we analyze in this study consists of the reservoir-induced microseismicity, a few local M2 earthquakes and some small to moderate regional earthquakes (M3 to M4 events located at >200 km from the field).

M2 Earthquakes

One of the pressing questions we aim to answer is what is causing these larger events. To be able to understand the causes we first need to improve these micro-earthquakes locations, magnitude estimates, focal mechanisms, and stress release. We obtain better source parameters when we include the accelerometer records to the dataset. Figure 2 shows an example of spectral modeling of SH waves of a Mw2.6 event using different sensor type data. The 3 sensors are located in the same observation well with the accelerometer at the surface and the 4.5 Hz and 15 Hz sensors right beneath it. We see that the event magnitude is underestimated when calculated from the short-period (geophone) data. The

magnitude scale based on short-period data alone, particularly if based only on the 15 Hz geophones data, tend to saturate at around M1.8. So, to more accurately estimate the magnitude of these larger events data with longer period signal is necessary.

The inclusion of the accelerometers with longer time window durations will also improve the locations of these larger events, and particularly of more distant events with longer S-P times, for which both P and S arrival times are now included in the record and can be used.

There are several proposed mechanisms that can generate these larger reservoir micro-earthquakes: gas extraction; reservoir subsidence; fluid induced; and static or dynamic triggering. Hydrocarbon production has long been correlated with reservoir induced seismicity (e.g., Segall, 1989). Reservoir depletion and loss of pressure along with subsidence is also a know mechanism of induced seismicity (e.g. Kovach, 1974; Segall et al., 1994). This is a strong hypothesis for the mechanism of these induced micro-earthquakes in this particular reservoir. Fluid injection increases the pore pressure and reduces the effective normal stress (Raleigh et al., 1976) facilitating the slip on micro-earthquakes close to failure. Depending on the micro-earthquake location relative to the injection well and on the degree of hydraulic connectivity in the reservoir, this could also be a possible mechanism. Static triggering by stress transfer is also an alternate mechanism that can explain induced seismicity (e.g., Gomberg et al., 1998; Rozhko 2010). Micro-earthquakes and injected fluid rearrange the local stress field promoting or preventing new micro-earthquakes in different regions and for certain fracture orientations. Finally, the dynamic triggering by the passage of seismic waves is also a possible mechanism. The larger reservoir events were first detected around April 2010. The hydrocarbon field is located in the Arabian tectonic plate near its boundary with the Eurasian plate, which runs over Iran. This plate boundary is seismically active with recently occurring large earthquakes and following aftershock sequences. In December 20, 2010 a M6.7 earthquake occurred SE of Bam, Iran; and three M6 earthquakes occurred in September 27, 2010, January 5th and 8th of 2011, NW of Shiraz, Iran (Figure 3). Induced seismicity triggered by the passage of seismic waves has been reported in many sites (e.g. Gomberg et al., 2001; Prejean et al., 2004; Brodsky, 2006), particularly in areas where fluids are present such as volcanic and geothermal areas. Some triggered earthquakes happen while the surface waves pass through a site, but others occur hours or even days later (Brodsky 2006). The micro-earthquakes may be close to failure and the passage of the seismic waves increases the effective stress on the fault just enough for it to fail. So one possibility to be investigated is if these >M2 reservoir events could have been dynamically triggered by the regional earthquakes.

The improved locations within the reservoir and relative to injection and extraction wells together with better source parameters will help discriminate between possible generation mechanisms of these larger reservoir micro-earthquakes.

Conclusions

We analyze –M3 to M3 seismicity related to a water flood injection program in a carbonate hydrocarbon reservoir at ~2 km depth recorded over a one year period. We improve the recording bandwidth or range of detectable events by integrating both a seismic network of vertical borehole arrays of geophones with longer period surface stations; this has the effect of extending the frequency content of the recorded signals. We obtained more accurate magnitude estimates for the larger events in the dataset and improved locations for more distant larger micro-earthquakes. We observe that earthquake magnitude scale saturates around M1.8 using traditional downhole geophone array configurations and suggest the inclusion of longer period sensors and adaptive time windows to better characterize the larger magnitude events. Using the improved source parameters we investigate the possible causative mechanism of the larger events.

References Cited

Brodsky, E., 2006, Long-range triggered earthquakes that continue after the wave train passes: Geophysical Research Letters, v. 33, p. L15313.

Gomberg, J., N.M. Beeler, and M.L. Blanpied, 1998, Earthquake triggering by static and dynamic deformations: Journal of Geophysical Research, v. 103, p. 24411-24426.

Gomberg, J., P. Reasenberg, P. Bodin, and R. Harris, 2001, Earthquake triggering by transient seismic waves following the Landers and Hector Mine, California earthquakes: Nature, v. 411, p. 462-466.

Kovach, R.L., 1974, Source mechanisms for Wilmington oil field, California subsidence earthquakes: Bull. Seismol. Soc. Am., v. 64, p. 699-711.

Kuleli, H.S., S. Sarkar, M.N. Toksoz, F. Al-Kindy, I.W. El Hussain, and S. Al-Hashmi, 2009, Monitoring Induced Seismicity at an Oil/Gas Field: American Geophysical Union, Fall Meeting 2009, abstract #S31E-03.

Li, J., H. Zhang, H. Kuleli, and N. Toksoz, 2011, Focal Mechanism Determination Using High Frequency Waveform Matching and Its Application to Small Magnitude Induced Earthquakes, Geophysical Journal International, v. 184, Issue 3, p. 1261-1274.

Prejean, S.G., D.P. Hill, E.E. Brodsky, S.E. Hough, M.J.S. Johnston, S.D. Malone, D.H. Oppenheimer, A.M. Pitt, and K.B. Richards-Dinger, 2004, Remotely triggered seismicity on the United States West Coast following the M7.9 Denali Fault earthquake: Bulletin Seismological Society of America, v. 94/6B, p. S348– S359.

Rozhko, A.Y., 2010, Role of seepage forces on seismicity triggering: Journal of Geophysical Research, v. 115, p. B11314.

Segall, P., 1989, Earthquakes triggered by fluid extraction: Geology, v. 17, p. 942-946.

Segall, P., J.R. Grasso, and A. Mossop, 1994, Poroelastic stressing and induced seismicity near the Lacq gas field, southwestern France: Journal of Geophysical Research, v. 99, p. 15423-15438.

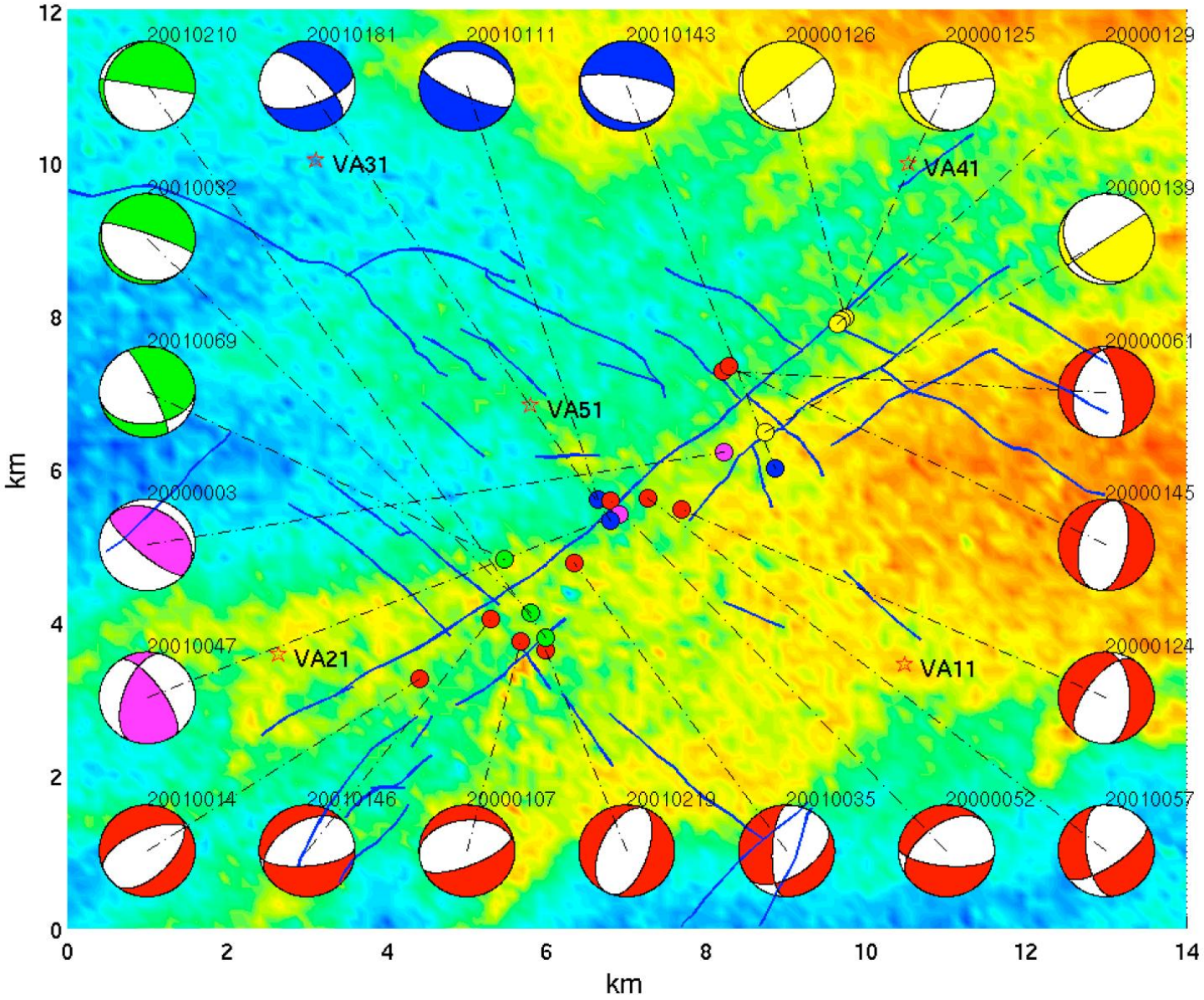

Figure 1. Hydrocarbon reservoir map showing the focal mechanisms of twenty two 2000/2001 events in the hydrocarbon field. The blue lines indicate the major faults and the map color indicates the local change in surface elevation with a maximum difference of about 10 m. Different focal mechanisms are grouped in several colors. (From Li et al., 2011).

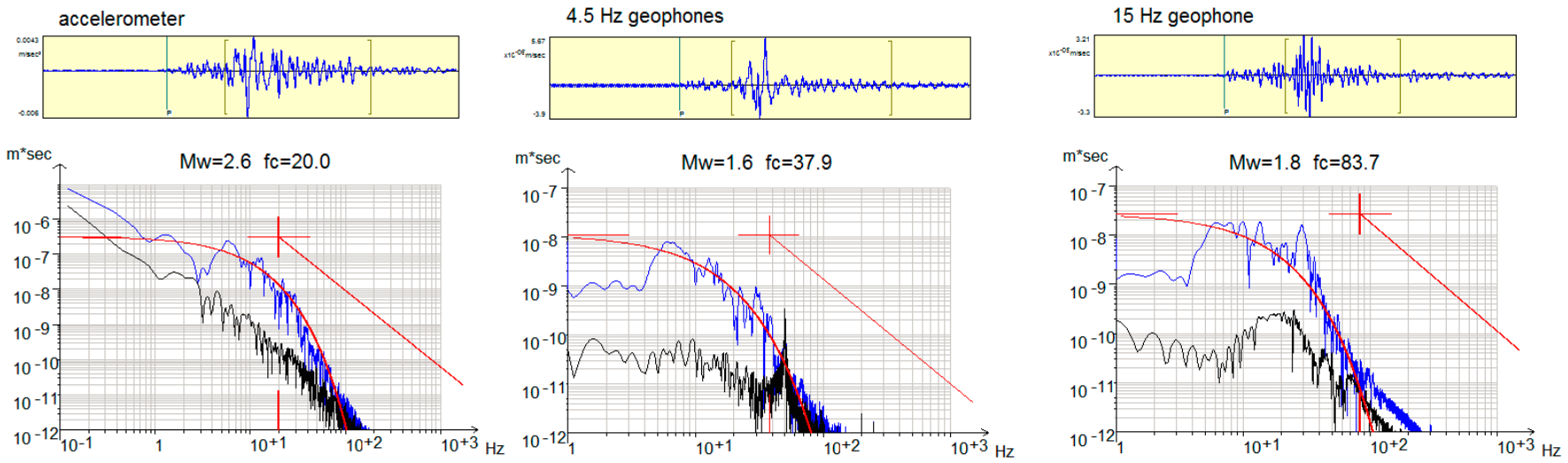

Figure 2. Spectral modeling of SH waves recorded at 3 different sensors: (left) accelerometer; (middle) 4.5 Hz geophone and; (right) 15 Hz geophone. Using geophone data alone underestimates the moment magnitude estimates for ~>M2 events. Accelerometer data gives a Mw estimate of 2.6. Q is held constant in the Mw calculations.

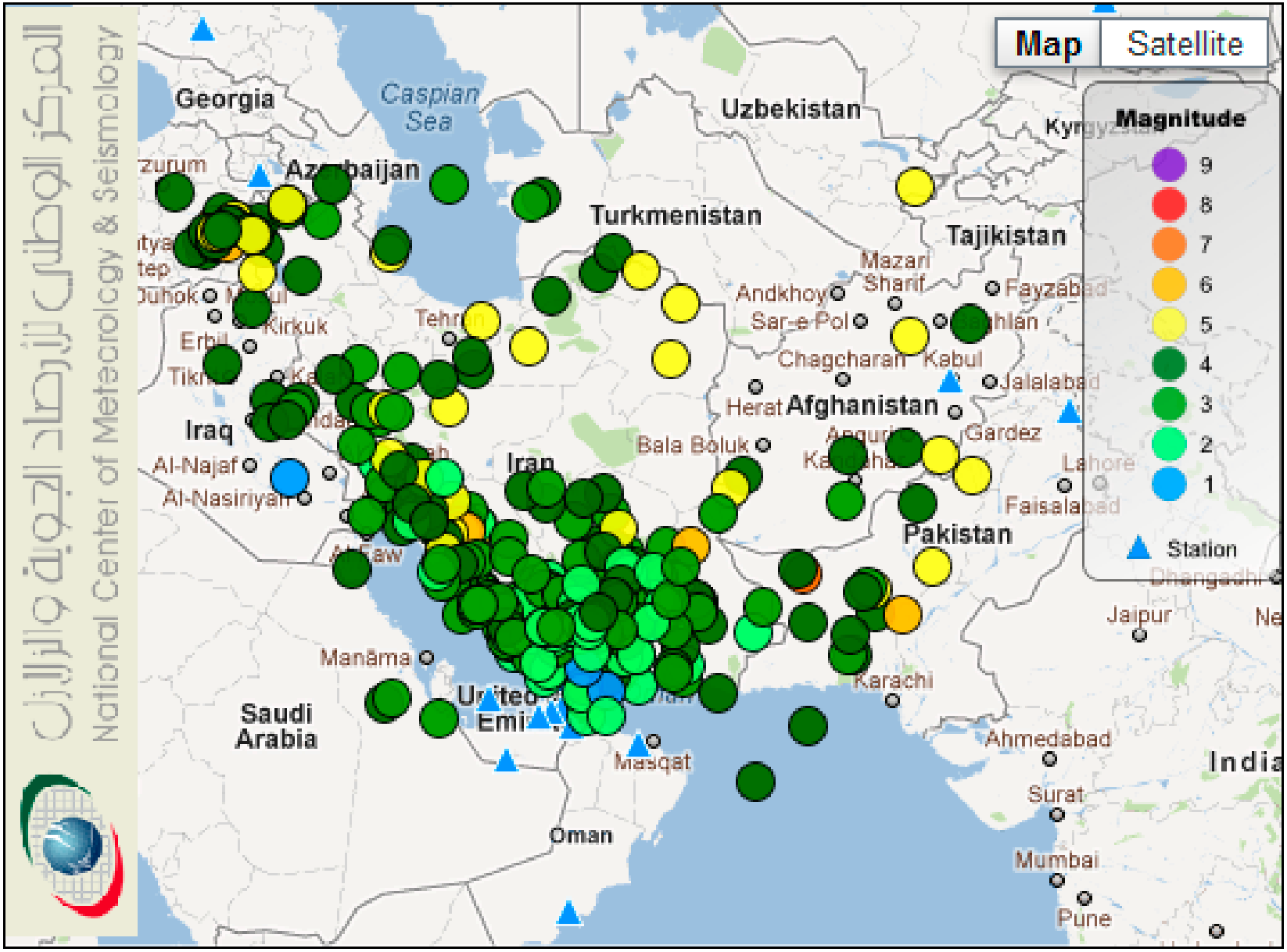

Figure 3. Regional seismicity map from January 2010 until February 2012.